Quantum Sensing and Information Processing

Lecture 2: Quantum Devices — Focus on LLNL Research

Steve Libby
Jonathan L DuBois

May 30, 2019

LLNL-PRES-778106

This work was performed under the auspices of the U.S. Department of Energy by Lawrence Livermore National Laboratory under contract DE-AC52-07NA27344. Lawrence Livermore National Security, LLC

Lawrence Livermore National Laboratory

Schedule Update

Quantum Devices
Thursday, May 30th at 2:00, B453 R1001, Armadillo Room

Application: Sensing with Quantum Devices
Thursday, June 27th at 2:00, B543 Auditorium, R1001

Control of Quantum Devices
Tuesday, July 2nd at 2:00, B132S R1000, GS/WCI Auditorium

Error Modelling
Tuesday, July 9th at 2:00, B543 Auditorium, R1001

Application: Quantum Computation
Tuesday, July 23th at 2:00, B543 Auditorium, R1001

https://casis.llnl.gov/seminars/quantum_information

Quantum Sensing: Detection, Interferometry, Noise* - *Requirements*!

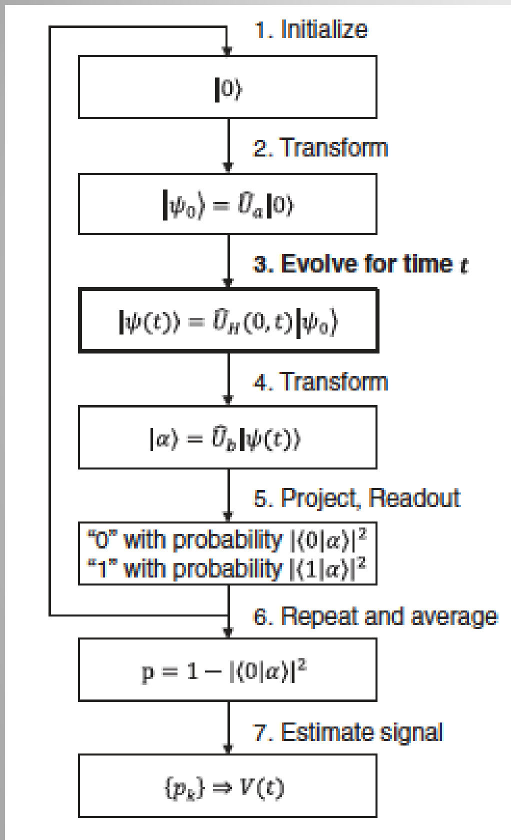

$$\hat{H}(t) = \hat{H}_0 + \hat{H}_V(t) + \hat{H}_{\mathrm{control}}(t)$$

Ramsey Interferometry

$$|\psi_0\rangle = |+\rangle \equiv \frac{1}{\sqrt{2}}(|0\rangle + |1\rangle) \rightarrow |\psi(t)\rangle = \frac{1}{\sqrt{2}}(|0\rangle + e^{-i\omega_0 t}|1\rangle) \rightarrow |\alpha\rangle = \tfrac{1}{2}(1 + e^{-i\omega_0 t})|0\rangle + \tfrac{1}{2}(1 - e^{-i\omega_0 t})|1\rangle$$

$$\begin{aligned} p &= 1 - |\langle 0|\alpha\rangle|^2 \\ &= \sin^2(\omega_0 t/2) = \tfrac{1}{2}[1 - \cos(\omega_0 t)] \end{aligned}$$

Quantum Projection Noise Limited Sensitivity

$$\delta F_{\min} = \frac{h\delta\varphi}{\mu T}$$

$$\delta F_{\min} = \frac{h\delta\varphi}{\mu T_2}\sqrt{\frac{T_2}{T}} = \frac{h}{\mu\sqrt{T_2 T N}}$$

Basic steps in the quantum sensing process

How does quantum noise limited sensitivity drive our 'quantum device' design?

Cold atom interferometry example

**Quantum sensing*, C. L. Degen, F. Reinhard, P. Cappellaro, RMP, 89, 035002, (2017).

Atomic Sensors – a review, J. Kitching, S. Knappe, E. A. Donley, IEEE Sensors, 11, 9, 1749, (2011).

Squeezed atomic states and projection noise in spectroscopy, D. J. Wineland, J. J. Bollinger, W. M. Itano, and D. J. Heinzen, Phys. Rev. A, vol. 50, pp. 67–88, (1994).

Laser Cooled Atoms and Quantum Coherence Give Rise to Sensitive Interferometers*

Laser cooling techniques are used to achieve the required velocity (wavelength) control for the atom source.

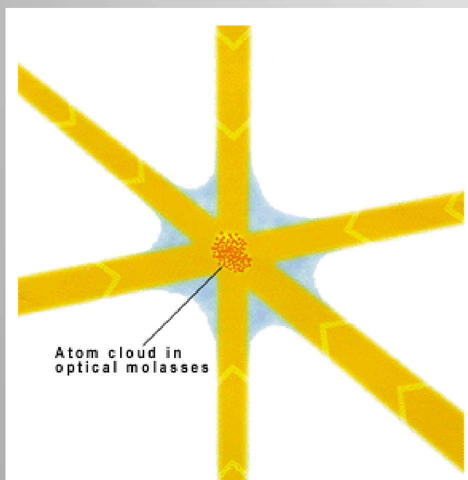

Image source:www.nobel.se/physics

Laser cooling: Laser light is used to cool atomic vapors to temperatures of $\sim 10^{-6}$ deg K.

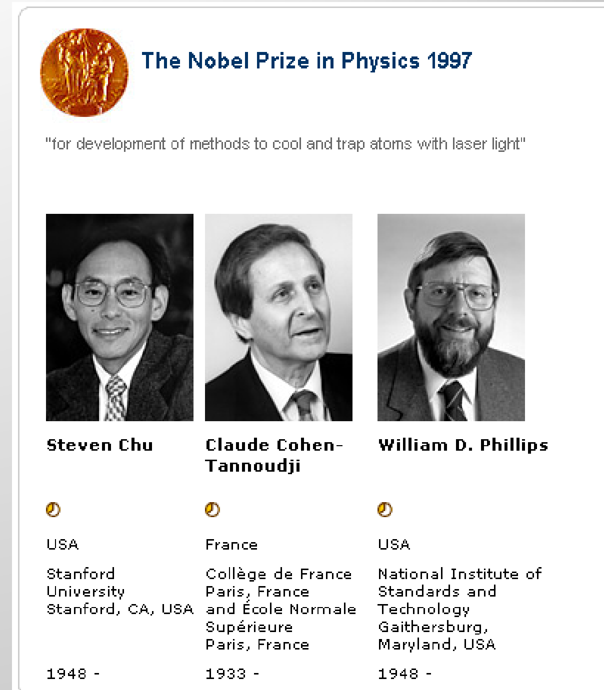

Laser Cooled Atoms Enable Sensitive Inertial Sensors – at 10^{-6} K, cesium de Broglie wavelength is $\sim h/(MkT)^{1/2} \sim .1\ \mu m$. (compare Overhauser's 1970's neutrons - $h/(mkT)^{1/2} \sim 1.445$ Å)

- *M. A. Kasevich and S. Chu, Phys. Rev. Lett. 67, 181, (1991) & Appl. Phys. B 54, 321, (1992)
- B. Young, M. Kasevich, and S. Chu, in Atom Interferometry, Academic Press, (1997)

Three key physics requirements for cold atom interferometry

- Laser cooling* : Doppler, polarization gradient, recoil limit
  - 2 level Doppler temperature limit (T ~ 125 μK for Cs)

$$k_B T_D = \frac{\hbar \Gamma}{2}.$$

  - Polarization gradient cooling / optical 'molasses.' (T ~ 2.5 μK)

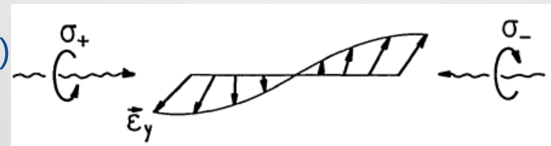

  - Recoil limit

$$k_B T_R = \frac{\hbar^2 k^2}{2M}$$

- Magneto Optical Trap*

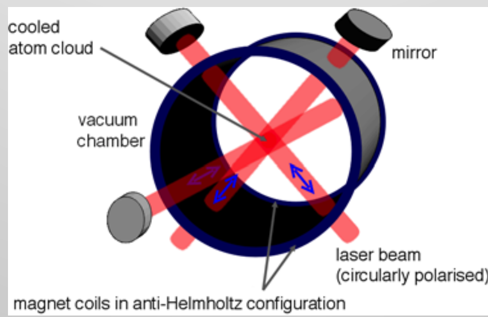

- Laser frequency and line width control
  - Roles of stabilization to < 10 MHz, 100 kHz, and 1 kHz.
  - Pound Drever Hall technique
- see J. Dalibard & C. Cohen-Tannoudji, JOSA B, (1989), 6, 11

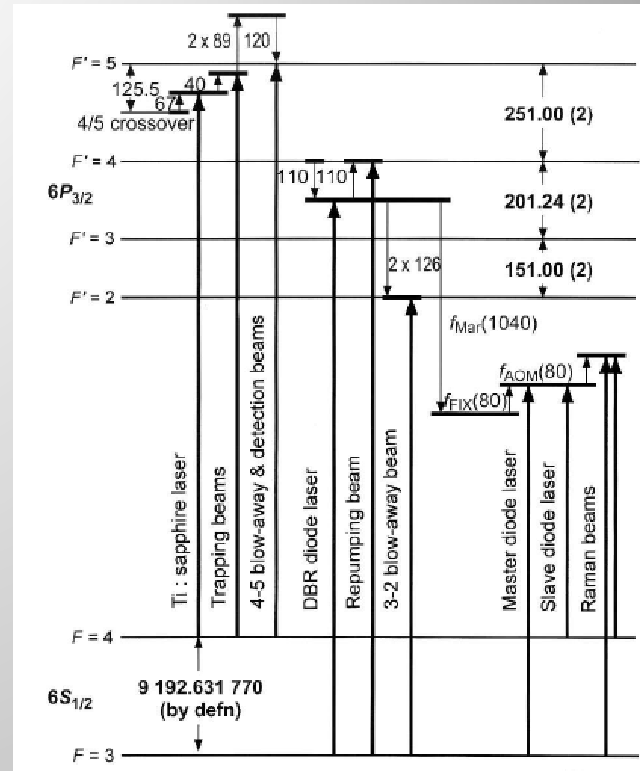

Figure 6. Atomic energy levels and laser frequencies. All laser frequencies are referenced either to the $F = 4 \leftrightarrow F' = 4 / F' = 5$ "crossover" resonance or the $F = 3 \leftrightarrow F' = 4$ resonance. Numerical values are in megahertz.

Key Cs transitions: Peters, Chung, and Chu, Metrologia, (2001), **38**, pp. 25-61.

* H. Metcalf and P. van der Straten, "Laser Cooling and Trapping," Springer, (1999).

(Light-pulse) atom interferometry builds on laser cooled atoms ($T \leq 10^{-6}$ K)

Resonant optical interaction

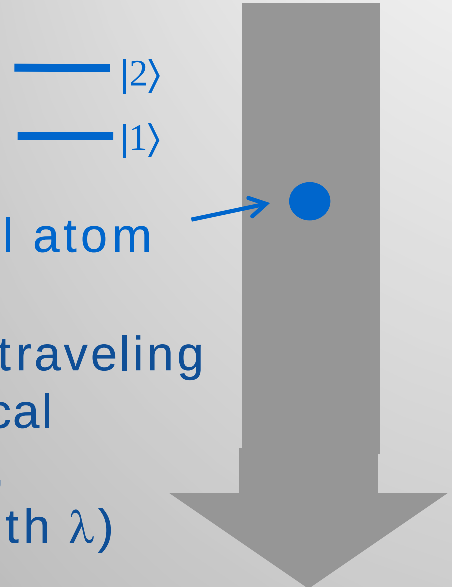

2-level atom

Resonant traveling wave optical excitation, (wavelength λ)

$$|\psi(t)\rangle = \cos\left(\frac{\Omega t}{2}\right)|1,\mathbf{p}\rangle + e^{-i\frac{\pi}{2}}\, e^{i\phi_L} \sin\left(\frac{\Omega t}{2}\right)|2,\mathbf{p}+\hbar\mathbf{k}_{\mathrm{eff}}\rangle$$

Recoil diagram

- Momentum conservation between atom and laser light field (recoil) leads to spatial separation of atomic wavepackets.

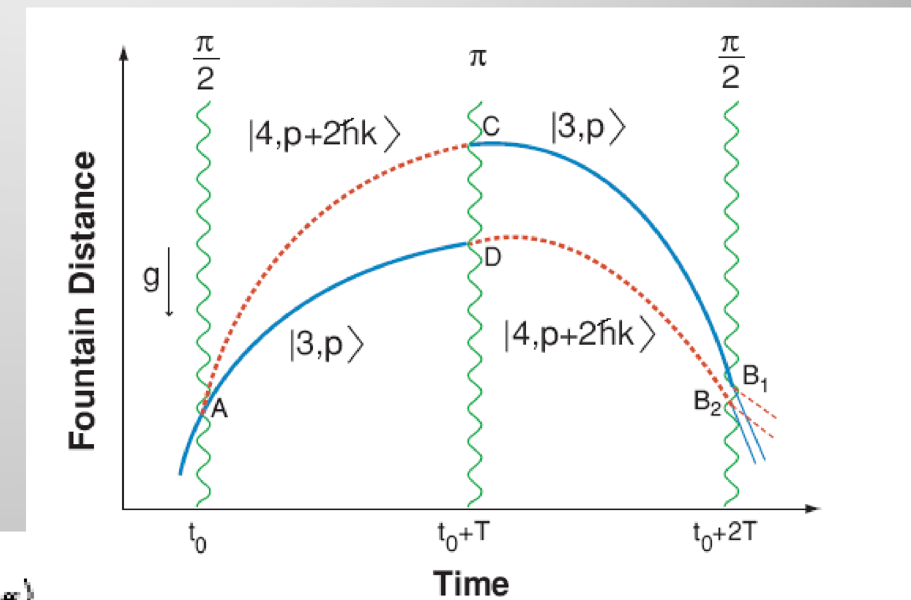

- 780 nm laser stabilized to < 1 kHz can measure the atom's position ~ 1:10^{12} .

Atomic deflection due to 25 kg mass at a distance of 1 meter over Δt ~ .25 sec is ~.5 Å.

- Semi-classical phase shift ~ $n\hbar k \delta g T^2$ High momentum transfer n >> 2.

Optically stimulated Raman transitions – Rabi oscillations between hyperfine states - advantages for quantum interferometry!

Level scheme

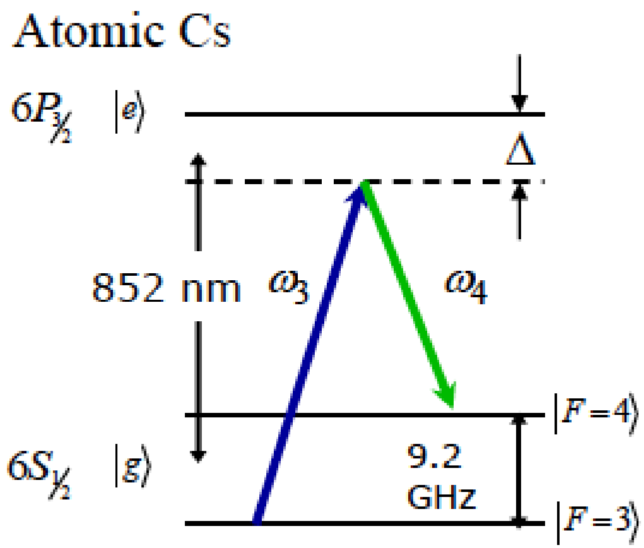

Excitation Geometry

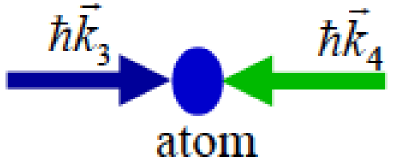

Doppler sensitive configuration

- $\mathbf{k_3}$, $\mathbf{k_4}$ counter-propagate

Ground states

- Avoid spontaneous emission
- Excitation between magnetic field insensitive sublevels

Large detuning D

- Effective 2-level system

  $F=3,\ m_f=0 \leftrightarrow F=4,\ m_f=0$
- Effective traveling wave excitation

  $\mathbf{k_{eff} = k_3 - k_4 \sim 2k_3}$
- Effective transition frequency

  $\Delta\omega_{eff} = \omega_3 - \omega_4$

Two Photon Raman Atomic Fountain Interferometer – Semi-classical Gravitational Phase Shift Analysis & Gradiometer Response

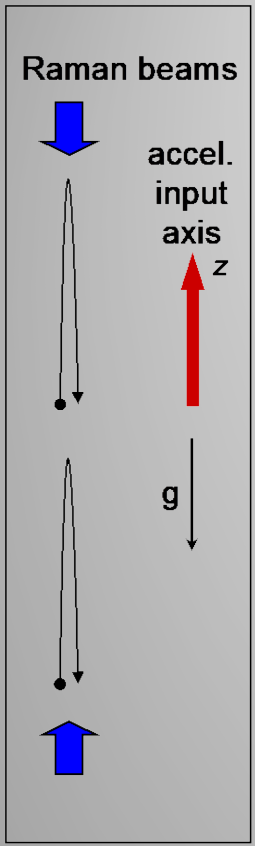

Paired atom fountains ‘interrogated’ by common Raman lasers

- Cooled, (initially F=3) cloud of ~ 10^8 alkali atoms. Unperturbed launch trajectory: v_0~ 2- 3 m/sec. t_1= 45 ms. T~ 250 ms. z_{02}-z_{01} ~ .5 m

$$\phi_{tm} = \vec{k}_{eff}\delta\vec{\phi},$$
$$\delta\vec{\phi} = \delta\vec{x}\left(t_1 + 2T\right) - 2\delta\vec{x}\left(t_1 + T\right) + \delta\vec{x}\left(t_1\right)$$

- Raman laser wavevector k_{eff} ~ 10^7 m^{-1}.

- Semiclassical treatment: Mach-Zehnder steps are in ‘sudden’ approximation. O(T^2) phase shift is solely due to light-atom interaction (k.δx) (higher order has Coriolis cross couplings, etc.)

$$\delta\vec{x}\left(t\right) = \int_0^t dt'\left(t - t'\right)\delta\vec{g}\left[\vec{x}_0\left(t'\right)\right]$$

- Individual interferometer gross phase ~ k_{eff} gT^2 ~ 10^8 radians (due mainly to the earth).

$$r\left(x\right) = \frac{\delta\phi_z^{(2)} - \delta\phi_z^{(1)}}{T^2\left(z_{02} - z_{01}\right)}$$

- Interferometer differences $\delta\varphi^{(1)}$-$\delta\varphi^{(2)}$: 1 to 10^{-4} rad. (10^{-3} rad ~ 2 10^{-9} /sec^2). Shot noise limited.

- Quantum corrections computed.

Ion traps: implementing controlled quantum logic

- Divincenzo quantum computing criteria met:
  - Scalable, well characterized qubits (e.g. ion hyperfine states in Wineland $^9Be^+$ scheme).
  - Ability to initialize to $|0000..\rangle$
  - Long decoherence time.
  - Universal gate set.
  - Qubit specific, quantum efficient measurement capability.

- Energy scales: ω_{recoil} ~ 50 - 250 kHz, ω_{axial} ~ 2-10 MHz, Ω_{Rabi} ~ .1 to 10 MHz, $\omega_{hyperfine}$ ~ 1.25 GHz ($^9Be^+$ S state), $\omega_{optical}$ ~ 729 nm ($^{40}Ca^+$)

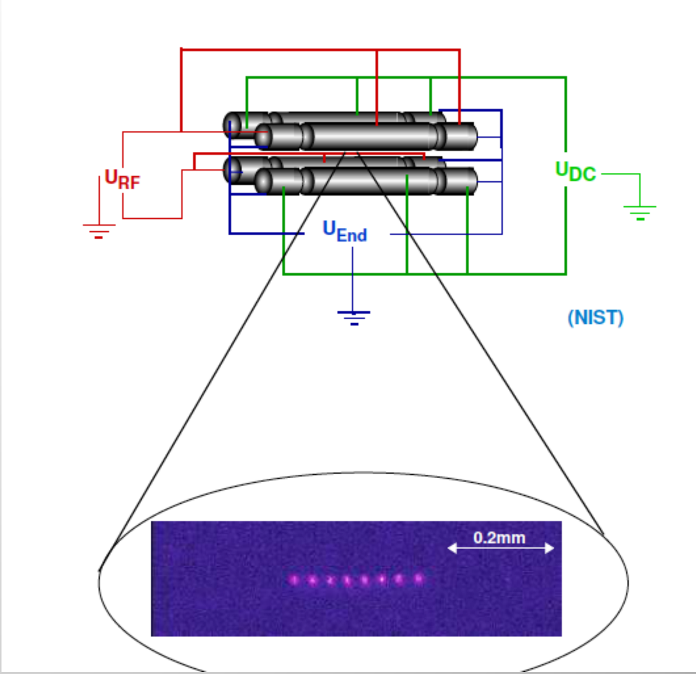

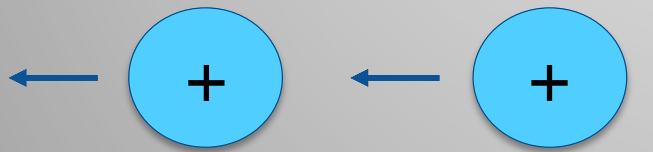

Laser Gradient: $\propto \eta\Omega$

$$\eta = k_z(\sqrt{\hbar / 2m\omega}) < 1$$

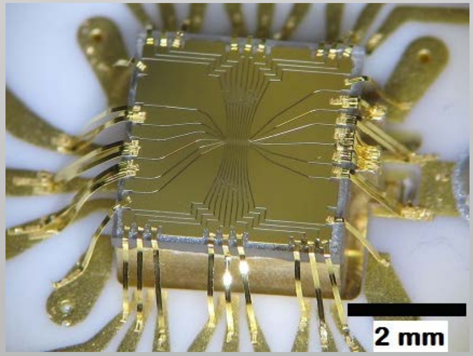

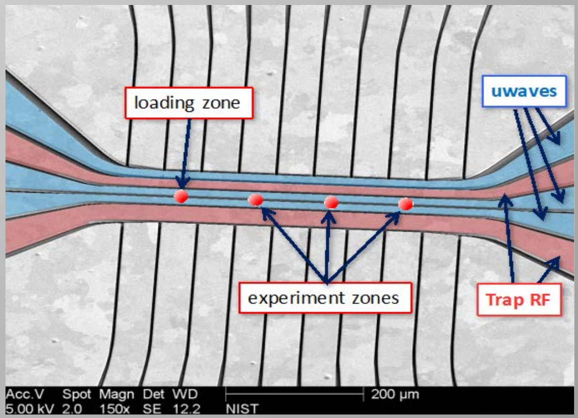

Ion trap quantum dynamics – effective Hamiltonians

$$H(t) = \overbrace{\underbrace{\frac{p^2}{2m} + \frac{m}{2}\omega_t^2 x^2}_{\text{harmonic oscillator}} + \underbrace{\frac{1}{2}\hbar\omega_a\sigma_z}_{\text{spin part}}}^{H_0} + \overbrace{\underbrace{\frac{1}{2}\hbar\Omega\left(\sigma^+ + \sigma^-\right)\left(e^{i(kx-\omega_l t+\phi)} + e^{-i(kx-\omega_l t+\phi)}\right)}_{\text{laser-ion interaction}}}^{H_1}$$

$$H = H_0 + H_{\text{int}}$$

$$H_0 = \nu(a^\dagger a + 1/2) + \omega_{eg}\sum_j \sigma_{zj}/2$$

$$H_{\text{int}} = \sum_j \frac{\Omega_j}{2}(\sigma_{+j}\ e^{i(\eta(a+a^\dagger)-\omega_j t)} + h.c.),$$

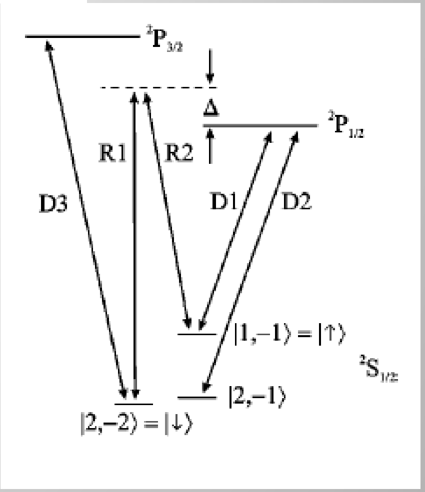

- Ion cooling analogous to neutral cold atoms –here Doppler cooling followed by 'phonon sideband' cooling.
- Wineland et. al. hyperfine qubit in $^9Be^+$ analogous to neutral alkali (Cs or Rb) ground state hyperfine dynamics.
- Blatt et. al. scheme in $^{40}Ca^+$ - qubit is on quadrupole transition.

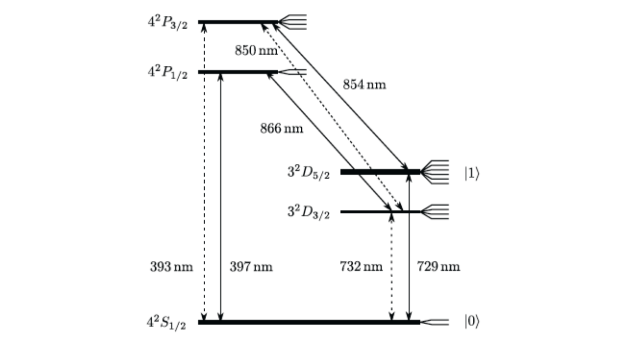

Figure 3.2 – *Atomic energy levels of $^{40}Ca^+$ with Zeeman substructure. The transitions indicated by solid arrows are driven by laser radiation during the experiment. The levels $S_{1/2}$ and $D_{5/2}$ are associated with the logical states $|0\rangle$ and $|1\rangle$. We use the standard atomic level notation $n^{2S+1}L_J$, where n is the principal quantum number, S is the spin angular momentum, L is the orbital angular momentum and J is the total angular momentum.*

Cirac-Zoller gate (1995) – universal, but requires cooling to motional ground state

- Couplings between qubits via phonon 'bus'
- Requires cooling to motional ground state.
- Laser couplings to side bands goes like Lamb-Dicke parameter (gradient).

Laser Gradient: $\propto \eta\Omega$

$$\eta = k_z(\sqrt{\hbar / 2m\omega}) < 1$$

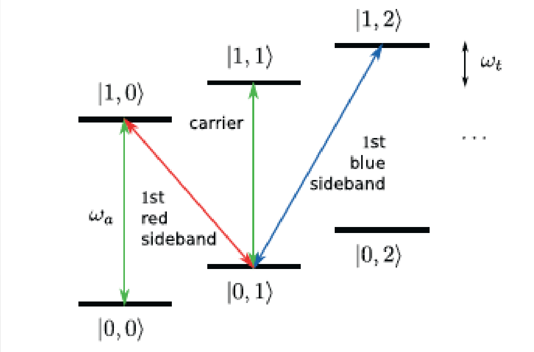

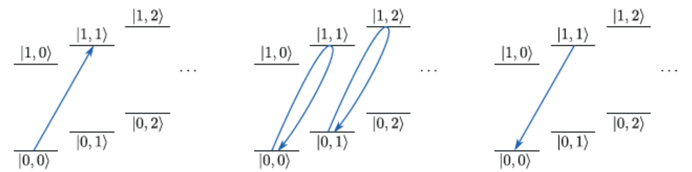

(a) First ion or control qubit: mapping to vibration.

(b) Second ion or target qubit: conditional phase acquisition

(c) First ion or control qubit: mapping from vibration to ion

Figure 3.6 – *Composite pulses scheme for a controlled phase gate. The internal state of the control ion is mapped to the vibrational quantum state (a), the target qubit acquires a phase flip (b) conditioned on the vibrational mode and the motion is mapped back to the control ion (c). Enclosed between two $\pi/2$-carrier rotations on the target qubit this gives a controlled-NOT gate.*

The development of the basis states goes according to

$$\begin{array}{lllllll} |0\rangle|0\rangle|0\rangle & \rightarrow & -i|1\rangle|0\rangle|1\rangle & \rightarrow & i|1\rangle|0\rangle|1\rangle & \rightarrow & -|0\rangle|0\rangle|0\rangle \\ |0\rangle|1\rangle|0\rangle & \rightarrow & -i|1\rangle|1\rangle|1\rangle & \rightarrow & i|1\rangle|1\rangle|1\rangle & \rightarrow & -|0\rangle|1\rangle|0\rangle \\ |1\rangle|0\rangle|0\rangle & \rightarrow & |1\rangle|0\rangle|0\rangle & \rightarrow & -|1\rangle|0\rangle|0\rangle & \rightarrow & -|1\rangle|0\rangle|0\rangle \\ |1\rangle|1\rangle|0\rangle & \rightarrow & |1\rangle|1\rangle|0\rangle & \rightarrow & |1\rangle|1\rangle|0\rangle & \rightarrow & |1\rangle|1\rangle|0\rangle. \end{array} \tag{3.28}$$

This realizes a controlled phase gate (up to a global phase factor of -1). To make this a controlled-NOT gate this sequence can be enclosed by a $R^{\mathrm{car}}(\frac{\pi}{2}, -\frac{\pi}{2})$ (beforehand) and a $R^{\mathrm{car}}(\frac{\pi}{2}, \frac{\pi}{2})$ pulse (afterwards).

The Mølmer-Sørensen (bichromatic) gate is ‘heat resistant!’

- MS-gate effective Rabi frequency is independent of the ion phonon occupation.
- Interference of different orderings of the ion excitation paths is key.
- Geometric phase gates similar (Milburn et. al.)
- Gate speed is an issue (optimality in the presence of differing noise sources)
- Magtraps vs. laser driven traps

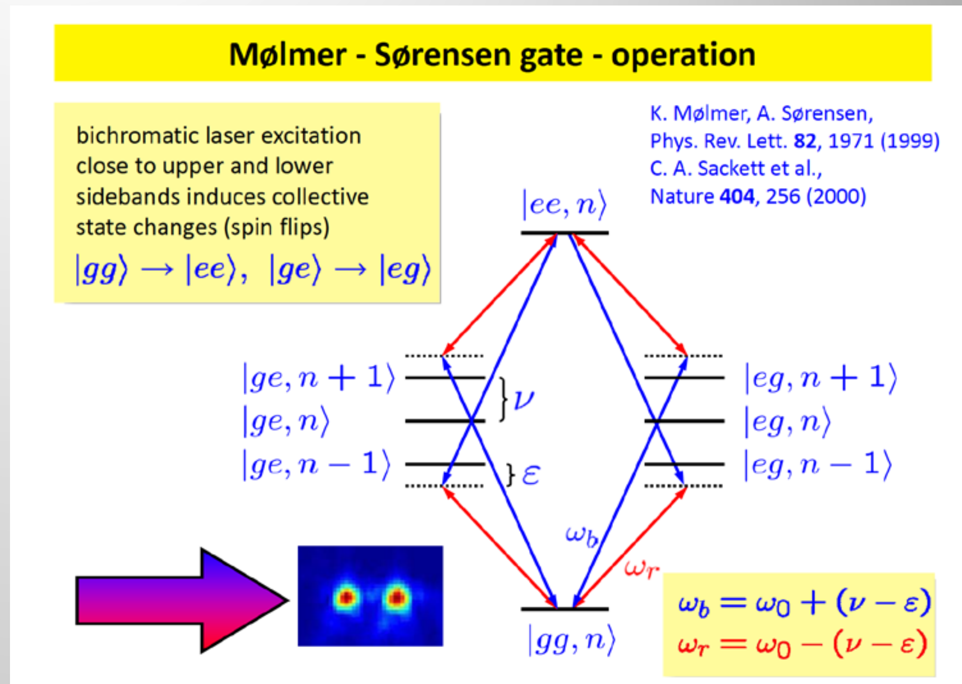

$$\left(\frac{\tilde{\Omega}}{2}\right)^2 = \frac{1}{\hbar^2}\left|\sum_m \frac{\langle een|H_{\rm int}|m\rangle\langle m|H_{\rm int}|ggn\rangle}{E_{ggn} + \hbar\omega_i - E_m}\right|^2$$

$$\tilde{\Omega} = -\frac{(\Omega\,\eta)^2}{2(\nu - \delta)}$$

Some General Quantum Sensing References – Also Cold Atoms

Quantum sensing – General

Quantum sensing, C. L. Degen, F. Reinhard, P. Cappellaro, RMP, 89, 035002, (2017).

Atomic Sensors – a review, J. Kitching, S. Knappe, E. A. Donley, IEEE Sensors, 11, 9, 1749, (2011).

Squeezed atomic states and projection noise in spectroscopy, D. J. Wineland, J. J. Bollinger, W. M. Itano, and D. J. Heinzen, Phys. Rev. A, vol. 50, pp. 67–88, (1994).

Cold Atoms / Atom Interferometry (I)

Laser Cooling and Trapping, H. Metcalf and P. van der Straten, Springer, (1999).

Atom Interferometry, Paul R. Berman ed., Academic Press, (1997).

Neutral atomic beam cooling experiments at NBS, Phillips, W. D., J. V. Prodan, and H. J. Metcalf,, in *Laser- Cooled and Trapped Atoms*, edited by W. D. Phillips (Natl. Bur. Stand, Washington, DC), Spec. Publ. 653, p. 1., (1983).

Laser cooling below the Doppler limit by polarization gradients: simple theoretical models, Dalibard, J., and C. Cohen-Tannoudji, 1989, J. Opt. Soc. Am. B **6**, 2023.

General Quantum Sensing References – Cold Atoms II

Three-dimensional viscous confinement and cooling of atoms by resonance radiation pressure, Chu, S., L. Hollberg, J. Bjorkholm, A. Cable, and A. Ashkin, Phys. Rev. Lett. **55**, 48., (1985).

Atomic motion in laser light, Cohen-Tannoudji, C., in *Fundamental Systems in Quantum Optics*, edited by J. Dalibard, J.-M. Raimond, and J. Zinn-Justin (North-Holland, Amsterdam), p. 1. (1992).

Atom Interferometry using stimulated Raman pulses, M. A. Kasevich and S. Chu, Phys. Rev. Lett. 67, 181, (1991).

Measurement of the gravitational acceleration of an atom, M. A. Kasevich and S. Chu, Appl. Phys. B 54, 321, (1992).

Precision Atom Interferometry with Light Pulses, B. Young, M. Kasevich, and S. Chu, in *Atom Interferometry*, Paul. R. Berman, ed., Academic Press, (1997).

High-precision gravity measurements using atom interferometry, A. Peters, K. Y. Chung, and S. Chu, Metrologia, (2001), **38**, pp. 25-61.

Matter – Wave Interferometers, A Synthetic Approach, C. J. Borde, in *Atom Interferometry*, Paul. R. Berman, ed., Academic Press, (1997).

Stepping back: ingredients for a quantum device

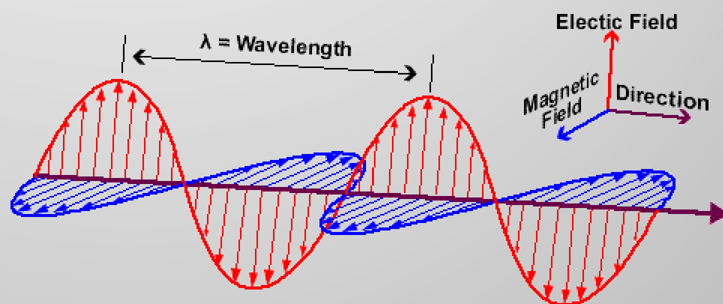

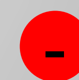

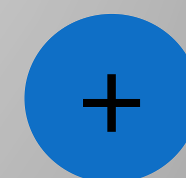

Quantum oscillators

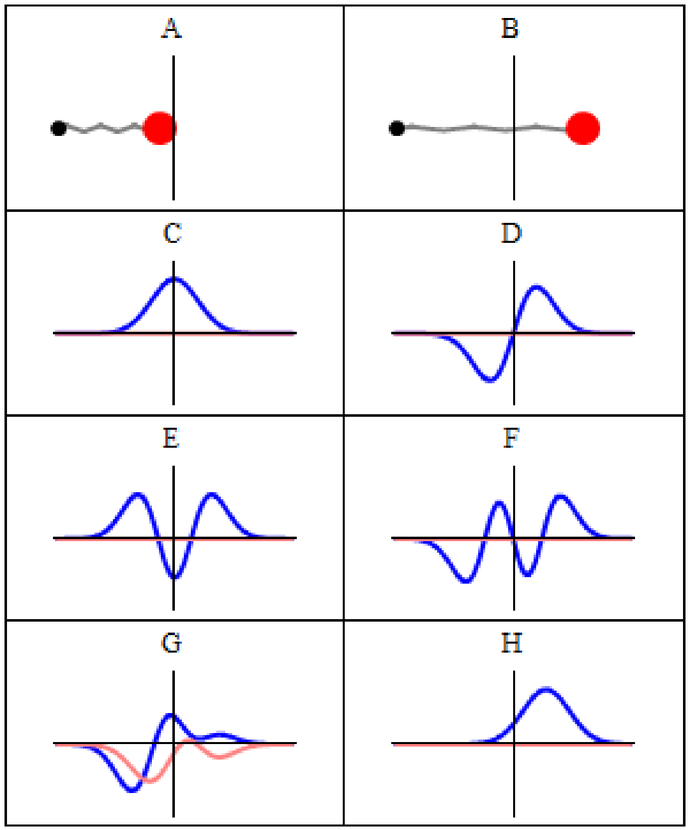

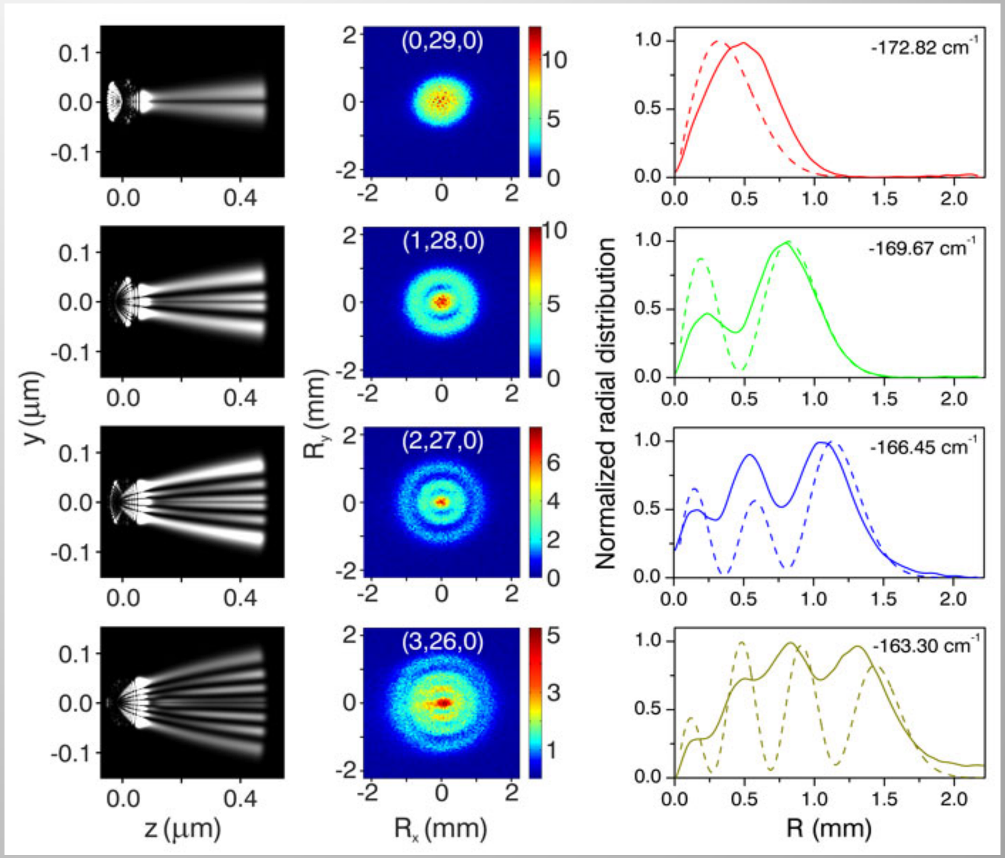

'Quantum microscope' peers into the hydrogen atom (Physics World 2013)

Quantum circuit oscillators?

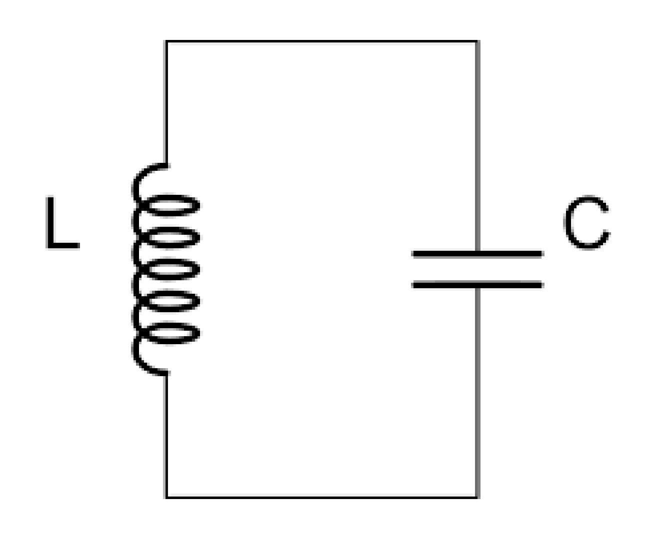

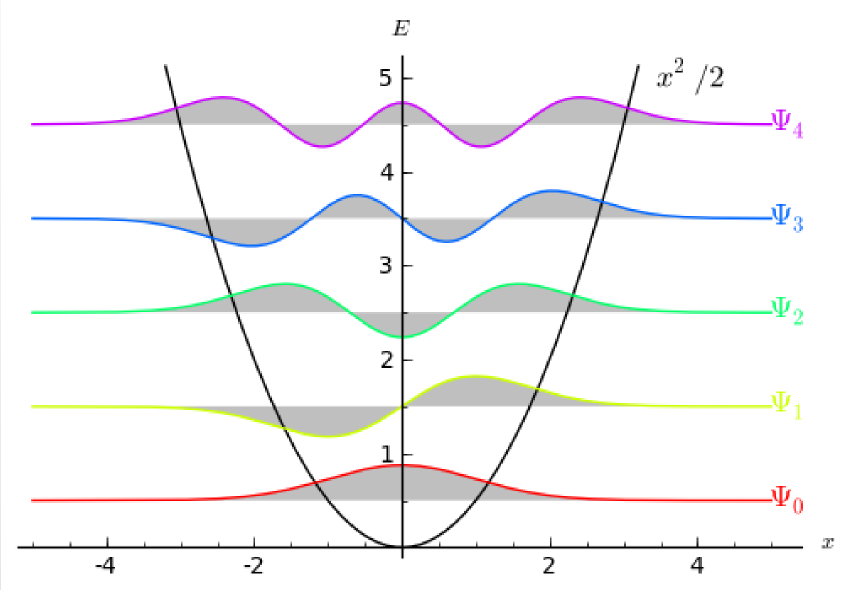

$$\omega_0 = \frac{1}{\sqrt{LC}}$$

Equally spaced energy levels

The importance of being nonlinear

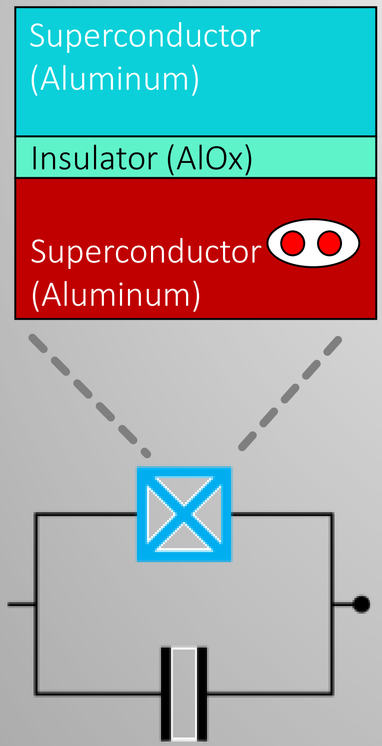

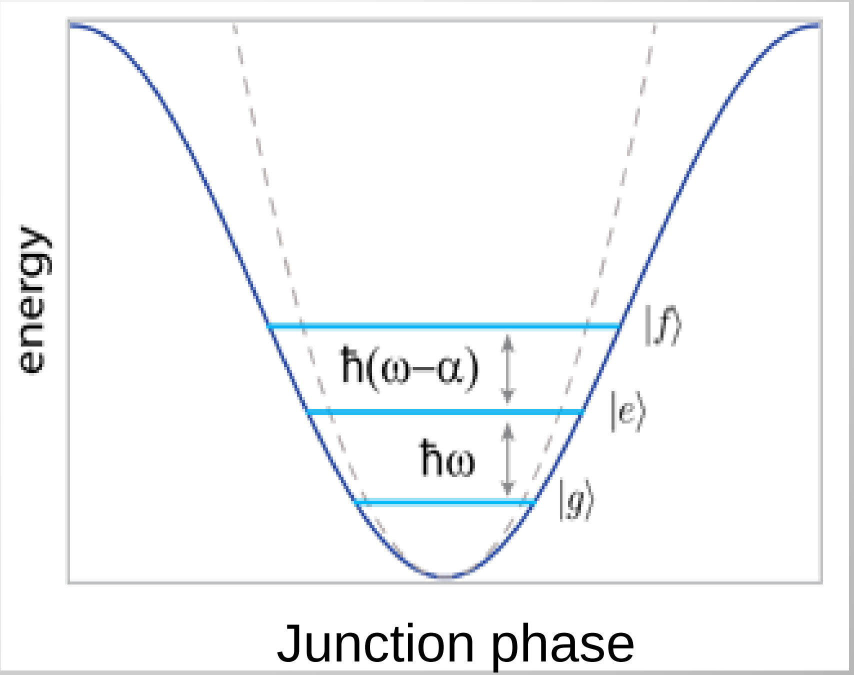

A Quantum Engineer's Guide to Superconducting Qubits
https://arxiv.org/abs/1904.06560
Introduction to quantum electromagnetic circuits
International Journal of Circuit Theory and Applications
Volume 45 Issue 7, July 2017

Scaling up from a single qubit

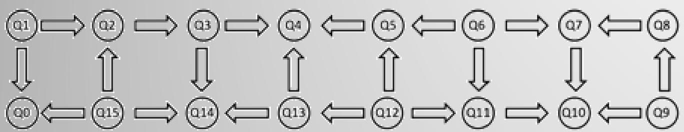

16-qubit backend: IBM Q team

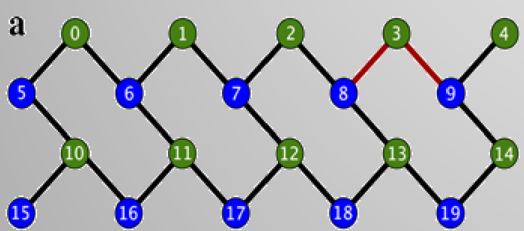

Connectivity of Rigetti 19Q

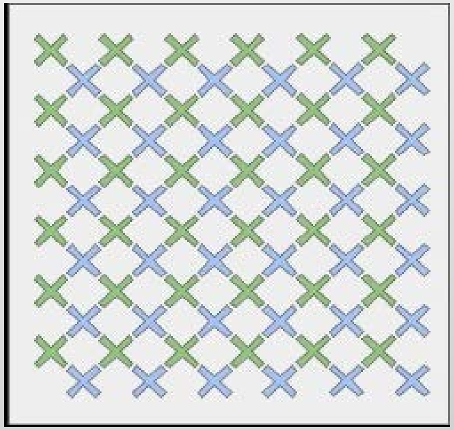

Google “Bristlecone” nearest neighbor layout

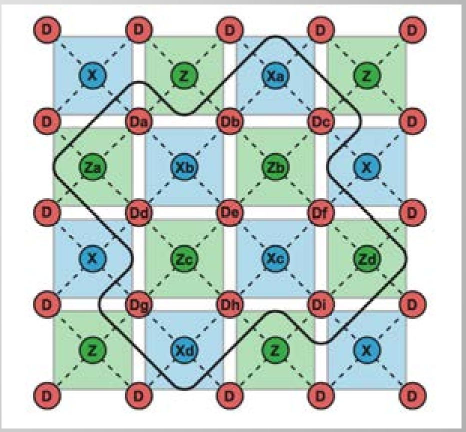

Layout of a surface-code fabric, Versluis et al.

Coulomb interaction is long range so underlying physical Hamiltonian is inherently nonlocal. Canonical design seeks to minimize ‘crosstalk’

Connectivity and Hilbert space traversal times

Typical undriven Hamiltonian for superconducting qudits / qubits:

$$H_0 \approx \sum_i^N \omega_i a_i^\dagger a_i - \chi_{ii} a_i^\dagger a_i^\dagger a_i a_i - \sum_{j \neq i}^N \chi_{ij} a_i^\dagger a_i a_j^\dagger a_j$$

Number of bosonic modes, N, determines number of qubits/qudits. Number of levels addressed, d, in each mode determines qudit size.

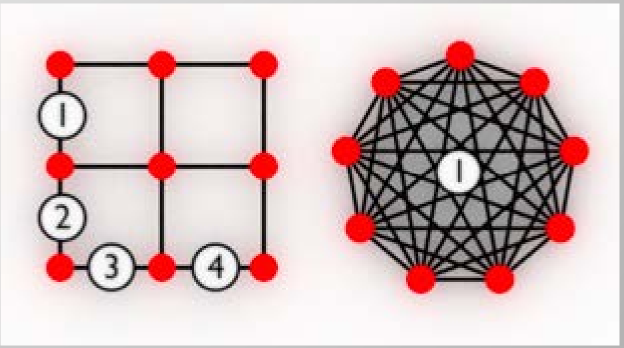

$$\omega_i \gg \chi_{ii} \gg \chi_{ij}$$

- Single qubit / qudit gates are fast
- Entangling gates are slower

H_0 *and* choice of gate set strongly influence connectivity / unit time

Qudits, Qubits and software-extensible quantum computing architecture

Qudits :: $SU(d)^N$

Qubits :: $SU(2)^N$

$$\begin{bmatrix}0\\0\\0\\\vdots\\0\end{bmatrix} \otimes \begin{bmatrix}0\\0\\0\\\vdots\\0\end{bmatrix}$$

$$\begin{bmatrix}0\\0\end{bmatrix} \otimes \begin{bmatrix}0\\0\end{bmatrix} \otimes \begin{bmatrix}0\\0\end{bmatrix} \otimes \cdots \begin{bmatrix}0\\0\end{bmatrix}$$

- Increasing d is a *control* problem: $f(t,\alpha)$
- Increasing N is a *hardware and fabrication* challenge: $\hat{H}_0$

Effective # of qubits = N $\ln_2(d)$

$$U(T;\alpha) = \int_0^T e^{it(\hat{H}_0 + f(t,\alpha)\hat{H}_c)} dt$$

Single control multiple qudit vs single qubit multiple control

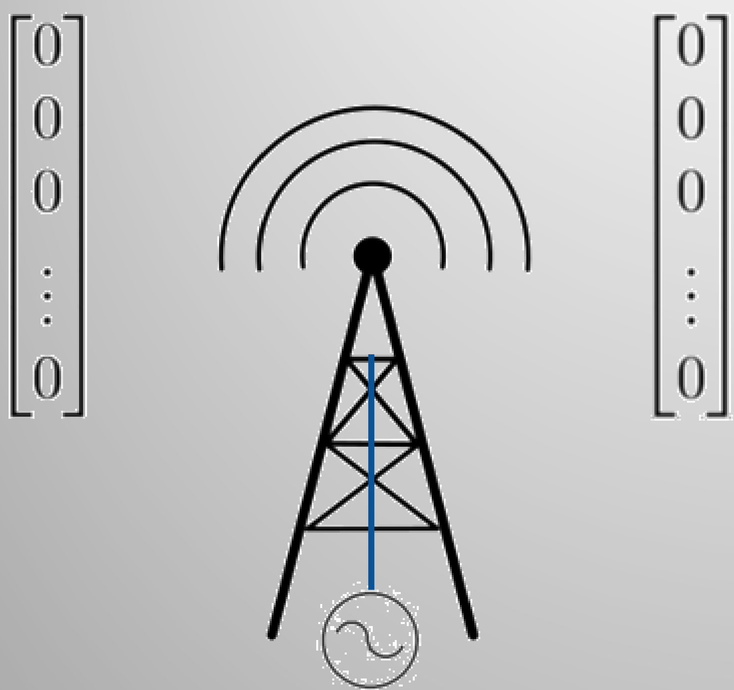

Single classical control line with frequency multiplexed signal drives all qudits.

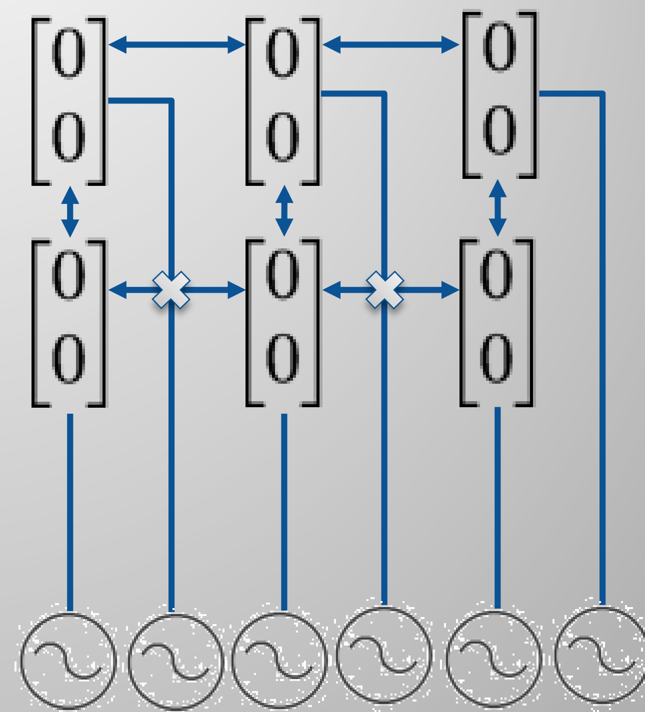

Multiple waveform generators drive individually connected qubits.

Control complexity, cost and fidelity bottlenecks are intertwined

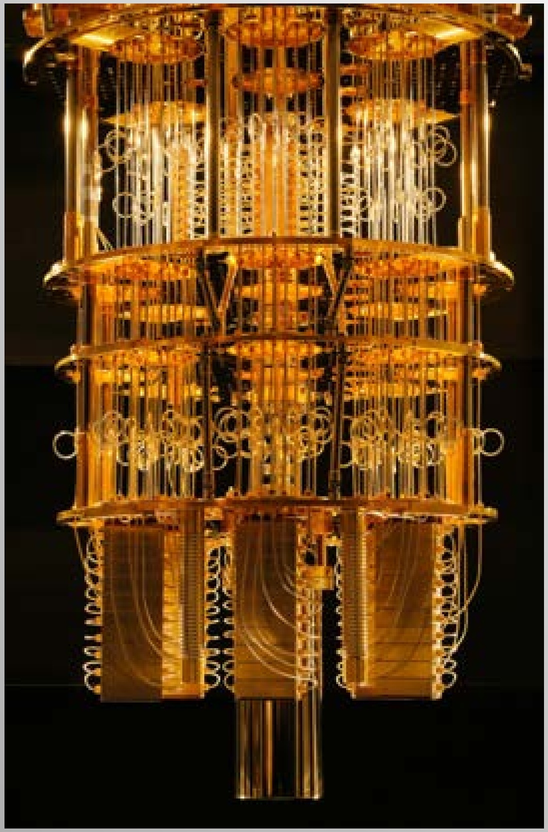

An IBM Q cryostat used to keep IBM's 50-qubit quantum computer cold in the IBM Q lab in Yorktown Heights, New York.

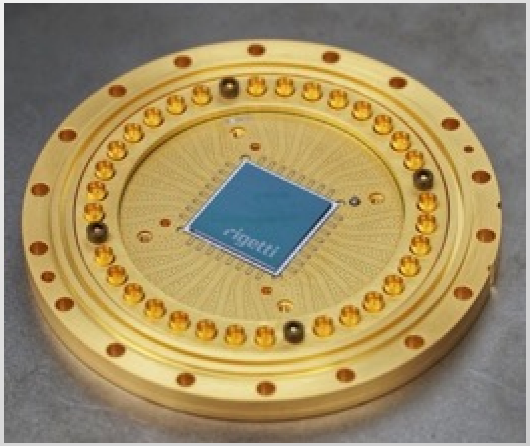

Rigetti Computing "Acorn" with RF connections.

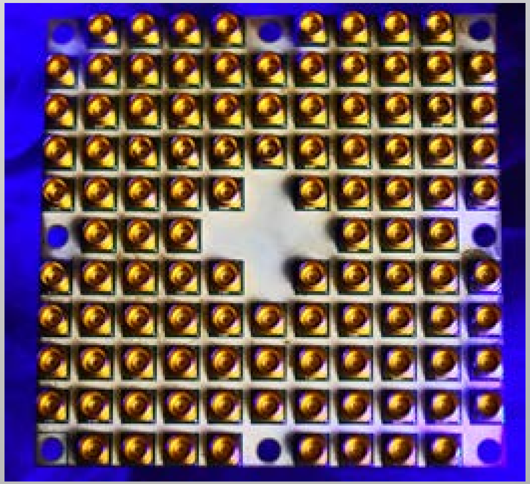

Intel 49 qubit quantum test chip "Tangle Lake," with RF connections.

Quantum device ==
Systems engineering problem

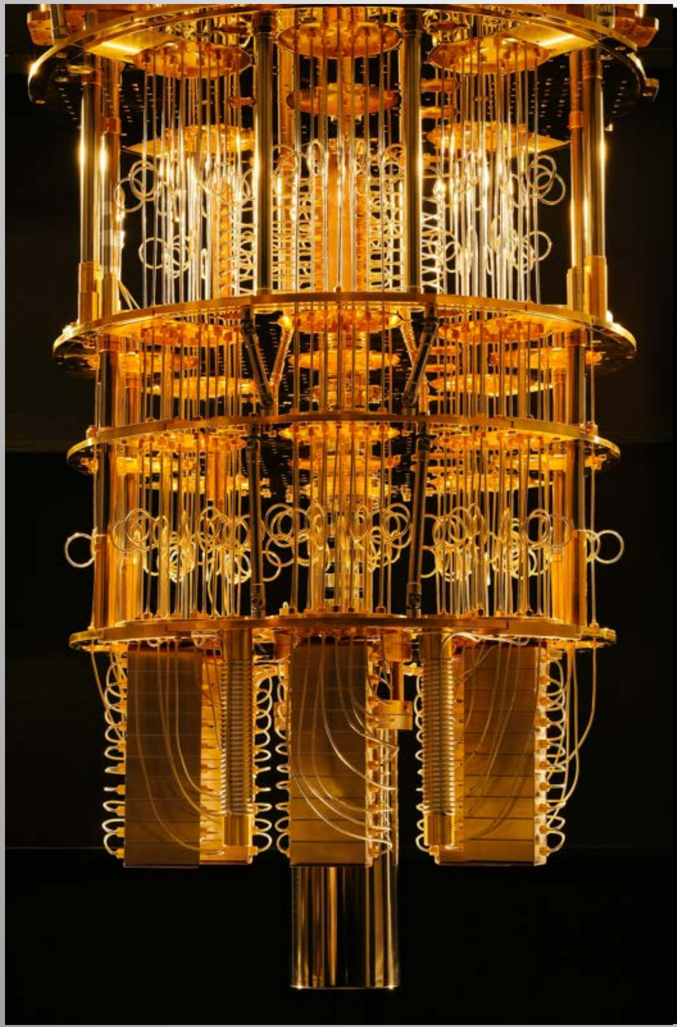

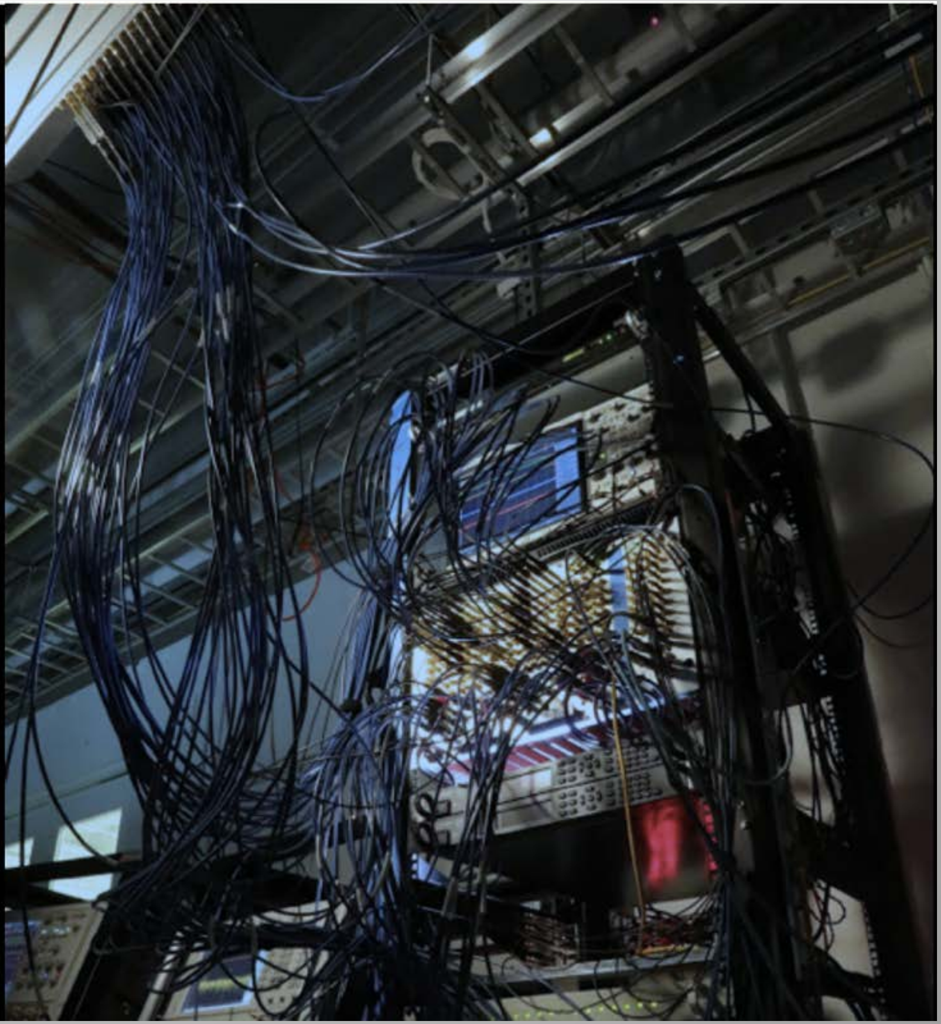

Systems challenges

High speed electronics

~Kilowatts 10^3 W

~Meters

300 K

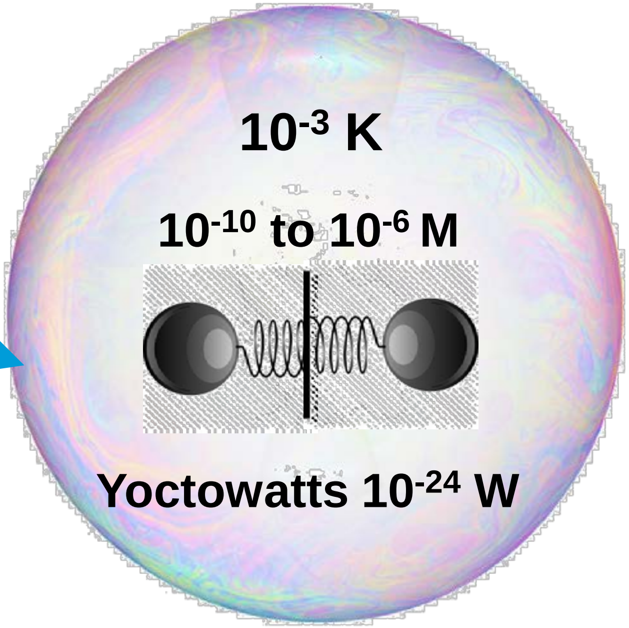

RF engineering / photonics

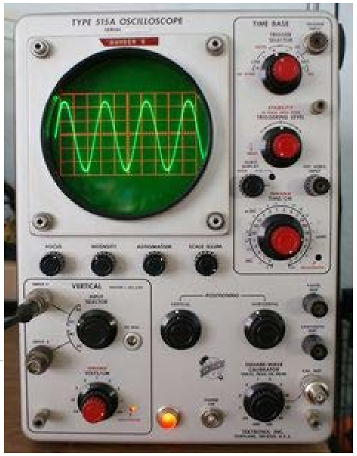

- Cryogenics
- High Vacuum
- Multiscale Materials
- Vibration isolation
- EM Shielding

- Quantum limited amplifiers
- Isolators / circulators
- Filters

Micro / nanofab, 3D integration

Back-up Slides—Quantum Sensors

Quantum Sensors*

TABLE I. Experimental implementations of quantum sensors.

Implementation	Qubit(s)	Measured quantity(ies)	Typical frequency	Initalization	Readout	Type[a]
Neutral atoms						
Atomic vapor	Atomic spin	Magnetic field, rotation, time/frequency	dc-GHz	Optical	Optical	II, III
Cold clouds	Atomic spin	Magnetic field, acceleration, time/frequency	dc-GHz	Optical	Optical	II, III
Trapped ion(s)						
	Long-lived electronic state	Time/frequency	THz	Optical	Optical	II, III
		Rotation		Optical	Optical	II
	Vibrational mode	Electric field, force	MHz	Optical	Optical	II
Rydberg atoms						
	Rydberg states	Electric field	dc, GHz	Optical	Optical	II, III
Solid-state spins (ensembles)						
NMR sensors	Nuclear spins	Magnetic field	dc	Thermal	Pick-up coil	II
NV[b] center ensembles	Electron spins	Magnetic field, electric field, temperature, pressure, rotation	dc-GHz	Optical	Optical	II
Solid-state spins (single spins)						
P donor in Si	Electron spin	Magnetic field	dc-GHz	Thermal	Electrical	II
Semiconductor quantum dots	Electron spin	Magnetic field, electric field	dc-GHz	Electrical, optical	Electrical, optical	I, II
Single NV[b] center	Electron spin	Magnetic field, electric field, temperature, pressure, rotation	dc-GHz	Optical	Optical	II
Superconducting circuits						
SQUID[c]	Supercurrent	Magnetic field	dc-GHz	Thermal	Electrical	I, II
Flux qubit	Circulating currents	Magnetic field	dc-GHz	Thermal	Electrical	II
Charge qubit	Charge eigenstates	Electric field	dc-GHz	Thermal	Electrical	II
Elementary particles						
Muon	Muonic spin	Magnetic field	dc	Radioactive decay	Radioactive decay	II
Neutron	Nuclear spin	Magnetic field, phonon density, gravity	dc	Bragg scattering	Bragg scattering	II
Other sensors						
SET[d]	Charge eigenstates	Electric field	dc-MHz	Thermal	Electrical	I
Optomechanics	Phonons	Force, acceleration, mass, magnetic field, voltage	kHz–GHz	Thermal	Optical	I
Interferometer	Photons, (atoms, molecules)	Displacement, refractive index	⋯			II, III

[a]Sensor type refers to the three definitions of quantum sensing in Sec. II.A.
[b]NV: nitrogen vacancy.
[c]SQUID: superconducting quantum interference device.
[d]SET: single electron transistor.

- Type I exploits quantum object (e.g. few state system with gaps).
- Type II exploits quantum phase coherence.
- Type III exploits 'true' quantum characteristics – entanglement/squeezing (non-classical correlations)

$$\psi = [2\cosh(2\theta)]^{-1/2} \times (e^{-\theta}|2\rangle_a|2\rangle_b + e^{i\phi}e^{\theta}|1\rangle_a|1\rangle_b)$$

- Atomic Clock – environment insensitive transition – lock local oscillator. (e.g. hyperfine $F = 4, m = 0\rangle$ to $F = 3, m = 0\rangle$)
- Field and force sensors – 'clock' operated on a sensitive transition.

* *Quantum sensing*, C. L. Degen, F. Reinhard, P. Cappellaro, RMP, 89, (2017), 035002.

How does 'Quantum Optic' Atom Interferometery Work - II?

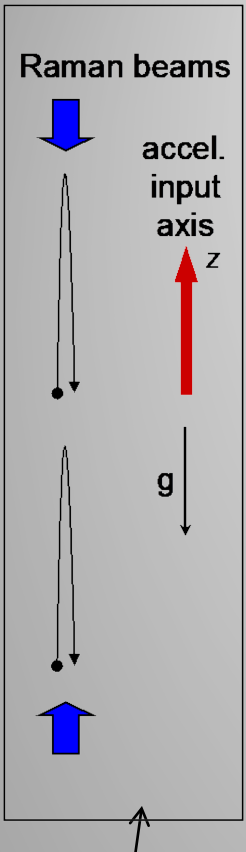

Paired atom fountains 'interrogated' by common Raman lasers – PINS gradiometer

Falling rock

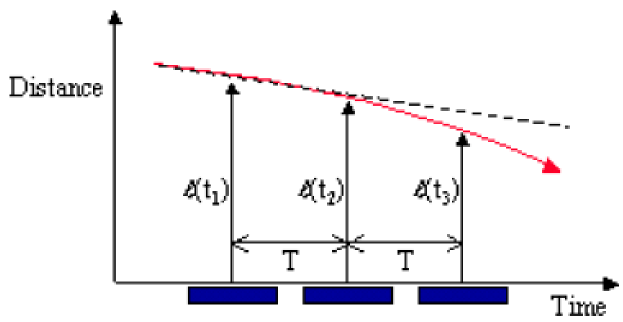

- Measure three distances: $\ell(t_1)$, $\ell(t_2)$ and $\ell(t_3)$
- Acceleration: $a \sim [\ell(t_1) - 2\ell(t_2) + \ell(t_3)]$

Falling atom

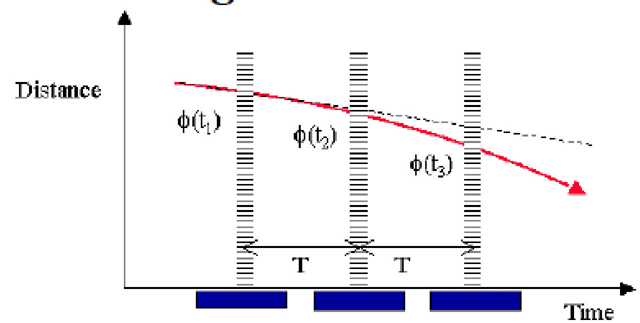

- Laser phases at atoms: $\phi(t_1)$, $\phi(t_2)$ and $\phi(t_3)$
- Atomic physics $\Rightarrow$ $a \sim [\phi(t_1) - 2\phi(t_2) + \phi(t_3)]$

Cold cesium atoms at ~ 1 μK (v ~ 1 cm/sec) are prepared in a magneto-optical trap in the F=3 state. The atoms are launched upward by moving optical molasses at v ~ 3 m/sec.

The two photon Raman method coherently splits and later recombines the cold cesium atoms in a quantum mechanical analog of a classical Mach-Zehnder interferometer.

780 nm laser stabilized to < 1 kHz can measure the atom's position ~ 1:10^{12}.

Atomic deflection due to 25 kg mass at a distance of 1 meter over Δt ~ .25 sec is ~.5 Å.

Cold-Atom interferometry gravity sensors demonstrate off-the-chart performance

AI sensor performance in open literature:

- Bias stability: $<<10^{-10}$ g
- Noise: $< 4\times10^{-9}$ g/Hz$^{1/2}$
- Scale Factor: $< 10^{-10}$

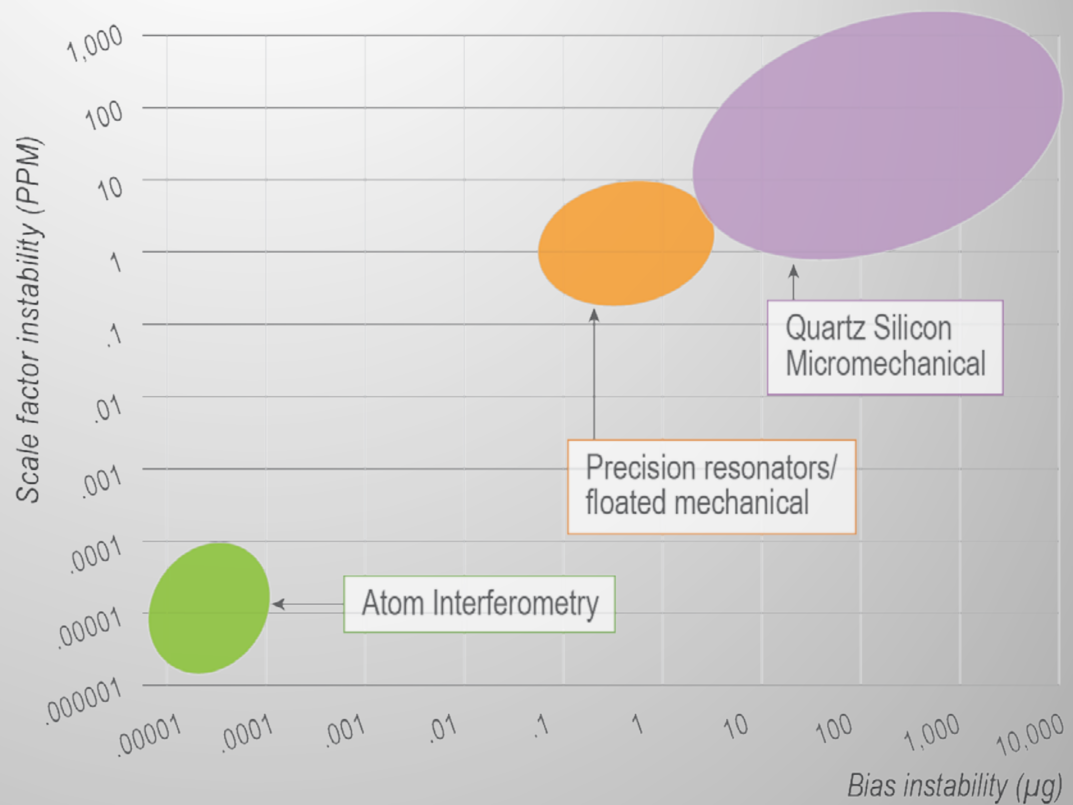

Bias – DC offset under zero applied acceleration

Scale factor – sensitivity relating applied acceleration to sensor output

Quantum projection noise limited performance (present) depends on *D, T,* number of atoms *N*, photon recoil k_{eff}, interference fringe contrast η:

$$\Delta T_{zz} \approx \frac{1}{\eta\sqrt{N}\, D\, k_{eff} T^2}$$

Squeezed state detection ~ $1/N^q$ (.5 < q < 1). Uncertainty limit ~ 1/N

Quantum Sensors Applications

- *Atomic Clocks*
  - Al^{+} , Yb, Sr, clock comparisons
- *Atomic fountain gravity gradiometry* (mass 'tomography')

  Hidden mass detection at close range (portal scan & emergency response) – (current LLNL/AOSense)

  Potential further applications: tunnel/underground structure detection, city building scan, treaty verification, …

  Closely connected to fundamental physics experiments:
  - Measure "G" to $1/10^{6}$
  - Space based sensors with ~ 10^{-5} E sensitivity – GRACE mission follow-on.
  - Gravitational wave detection in the .1 – 10 Hz regime
  - 'high momentum transfer'
- *Inertial motion sensors* – beyond GPS – dead reckoning navigation (current AOSense/LLNL)

  Navy and Air Force navigation

  High precision navigation solution – Machine learning improved Kalman filter.